

See discussions, stats, and author profiles for this publication at: <https://www.researchgate.net/publication/275222228>

High-order harmonic generation during propagation of the double-pulse beam through the drilled thin films

ARTICLE *in* APPLIED PHYSICS A · JUNE 2015

Impact Factor: 1.7 · DOI: 10.1007/s00339-015-9160-x

READS

28

4 AUTHORS, INCLUDING:



Rashid Ganeev

Saitama Medical University

404 PUBLICATIONS 4,287 CITATIONS

SEE PROFILE



Masayuki Suzuki

Saitama Medical University

167 PUBLICATIONS 2,539 CITATIONS

SEE PROFILE

High-order harmonic generation during propagation of the double-pulse beam through the drilled thin films

Rashid A. Ganeev¹ · Masayuki Suzuki¹ · Shin Yoneya¹ · Hiroto Kuroda¹

Received: 9 March 2015 / Accepted: 31 March 2015 / Published online: 8 April 2015
© Springer-Verlag Berlin Heidelberg 2015

Abstract High-order harmonic generation using the femtosecond pulses propagating through the thin (~ 0.1 mm) drilled films is demonstrated. The harmonics were observed in the case of double-pulse beams while using various films (Mo, In, polyethylene, paper). The harmonics up to the 25th order were generated during propagation through the drilled polyethylene film. The simplicity, absence of additional source of heating radiation, and artificial optimization using the adjustment of the double pulses have shown the possibility in application of this technique for the high-order harmonic generation in thin ablated films.

1 Introduction

A search for new methods of high-order harmonic generation (HHG) using ultrashort pulses has long been among the important topics of the nonlinear optical studies. Alongside the commonly used techniques of harmonic generation in isotropic media such as gases [1, 2] and plasmas [3–5], the use of thin films has been considered a versatile approach for lower-order harmonic generation in the near-ultraviolet region.

The researchers took the advantage of small absorption in these thin films, which allowed the study of harmonics up to the fifth order of the near-infrared laser sources. Low-order nonlinear optical conversion has previously been studied in various thin films of wide-bandgap materials.

Particularly, very high conversion efficiency of the third-harmonic radiation was achieved in a submicron-thick film of a nanocrystalline ZnO deposited on a fused silica substrate [6]. It was shown that the nonresonant nonlinear optical susceptibilities of these materials may be significantly affected by the small sizes of nanocrystals. They reported the efficient third-harmonic generation (THG) in thin films of ZnO leading to direct generation of UV light from the femtosecond laser generating in the 1200–1300 nm range. THG in ZnO thin films was also reported in Ref. [7]. In Ref. [8], the quasi-phase-matched second-harmonic generation (SHG) with conversion efficiency of 10^{-6} – 10^{-5} was analyzed while using the periodic stack of free-standing polymer films. SHG and THG in single-wall carbon nanotube layers and methacrylate films produced by low-velocity spraying were studied in Refs. [9, 10] using the 75-fs pulses of Cr/forsterite laser radiation. Harmonic generation processes are shown to be ideally suited for the nonlinear spectroscopy and structure analysis of these species. The third-harmonic intensity, scaling as a cubic function of the pump pulse intensity up to the laser breakdown threshold, is substantially increased under conditions of optical breakdown. This finding suggests the third harmonic as a convenient probe for the online monitoring of optical breakdown in transparent materials.

It is clear that, in order to achieve high conversion efficiency, one has to increase the incident intensity of the laser and use materials with the highest possible nonlinear optical susceptibility. An increase in the incident laser intensity above a certain threshold level will damage samples under study and lead to the ablation of the material. At the same time, the ablation technique has already been exploited in the case of thin films to generate lower-order harmonics. In Ref. [11], ultrasmall CdS particles were

✉ Rashid A. Ganeev
rashid_ganeev@mail.ru

¹ Ophthalmology and Advanced Laser Medical Center,
Saitama Medical University, Saitama 350-0495, Japan

embedded in polyvinyl alcohol films and ablated by 308 nm laser. THG at these conditions was obtained for various sizes of CdS particles, and the optical nonlinearity in the nonresonance region was found to remain almost constant in the diameter range studied. Meanwhile, the shift toward the shorter wavelength range is restricted by the limitations caused by the absorptive properties of films. This limitation is a main restricting factor during the HHG studies in the bulk materials. To overcome this problem, one has to considerably reduce the concentration of the medium, particularly using a laser ablation technique.

The method we propose is based on the ablation of thin films during their drilling by the ultrashort pulses. The ablation by single pulse causes strong plasma emission followed with the appearance of tiny drilled hole. However, once the plasma becomes less dense, either by introducing longer delay between the ablation pulse and second pulse or by using already existing tiny hole in the material, the following pulse can cause the generation of high-order harmonics in the newly prepared low-excited plasma medium. The principles of HHG in the extreme ultraviolet (EUV) range are based on the same approach, which has been used in the case of gas and plasma HHG. The three-step model [12] allowed the explanation of main experimental findings of the HHG by different means. In this paper, we demonstrate, for the first time to our knowledge, the HHG using the double pulses propagating sequentially through the preliminary formed tiny hole in different thin (~ 0.1 mm) films.

2 Experimental arrangements

The radiation of Ti/sapphire laser (central wavelength 802 nm, pulse duration 70 fs, pulse energy $E_{fp} = 4$ mJ, 10 Hz pulse repetition rate) was focused using the 400-mm-focal-length spherical lens on the thin solid targets placed in the vacuum chamber (Fig. 1a). The intensity of driving pulse at the focus area was varied up to 8×10^{14} W cm $^{-2}$. The targets (thin metal films, paper, and polyethylene film) were inserted in the focal plane of the focusing lens using the translation stage to create the conditions when the ultrashort pulse drills the hole in these targets. The plasma emission was analyzed using the EUV spectrometer after a few shots leading to the hole formation. Further shots created less dense plasma by the wings of the spatial distribution of the ultrashort pulses and did not lead to the harmonic generation since the temporal separation between the two pulses at 10 Hz pulse repetition rate (100 ms) was too long to maintain the plasma plume at the axis of drilled hole at the moment of propagation of the following laser pulse.

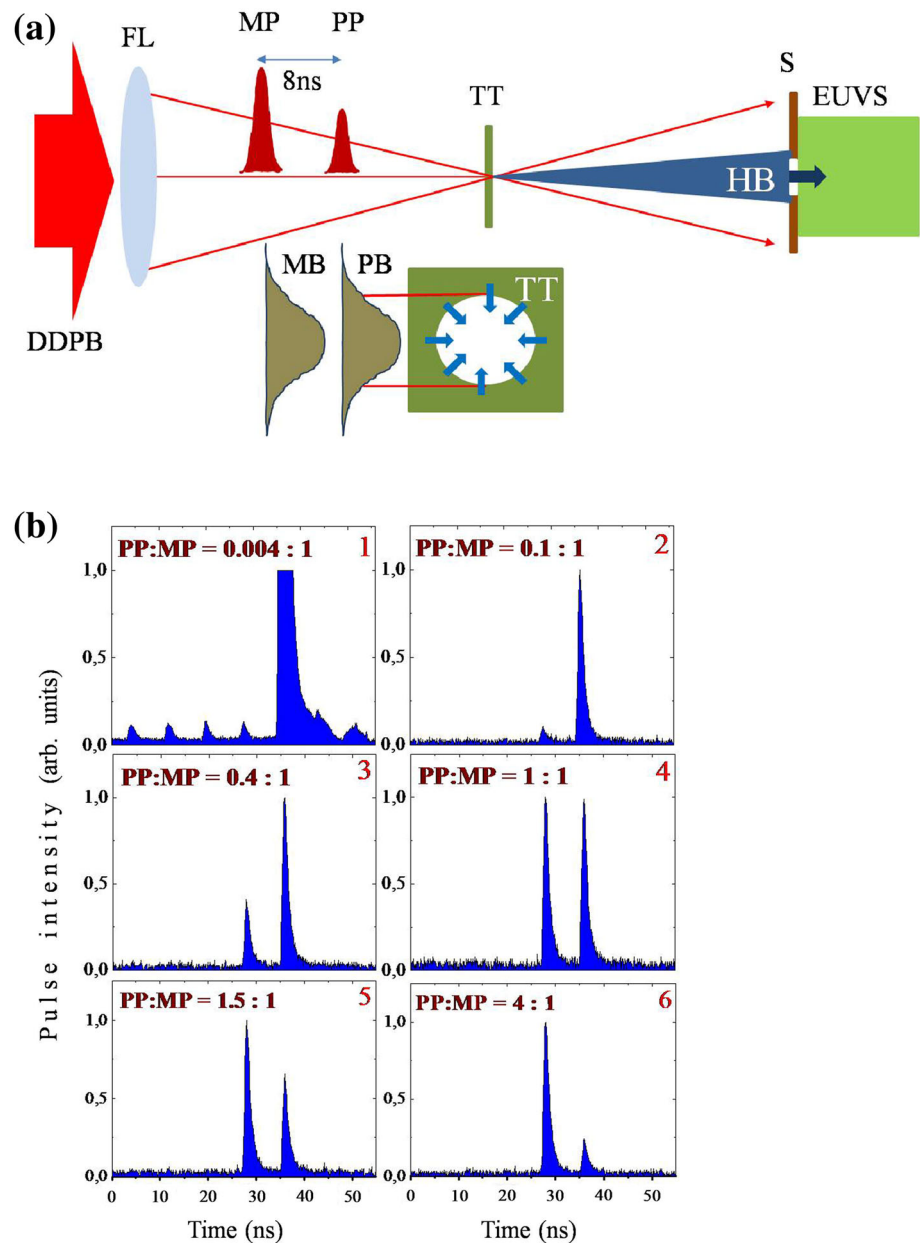
The conditions of plasma formation and laser–plasma interaction were significantly changed once we introduced the double-pulse scheme. The double-pulse beam was produced by tuning the triggering signal on the Pockels cell of the regenerative amplifier (TSA-10, Spectra-Physics Lasers) of Ti/sapphire laser. Usually, the train of generated pulses from this amplifier was used for separation of a single pulse from the maximally amplified pulses of this train. The variation of the delay of the triggering signal on the driver of Pockels cell allowed separation of double pulses with the 8 ns time interval. We were able producing two driving pulses (double-pulse scheme) with variable ratio between the intensities of these pulses. Panel 1 of Fig. 1b shows the conditions when single pulse was separated from the train, which demonstrate the reasonably high contrast of main pulse (MP) with regard to other pulses of the train. The ratio of pre-pulses and main pulse (PP/MP) in that case was 4×10^{-3} . The intensity of these pre-pulses did not allow plasma formation during interaction of the wings of the spatial distribution of these pulses and the edges of hole.

3 Results and discussion

Once we gradually changed the delay of the triggering pulse on the Pockels cell, the neighboring pre-pulse with variable intensity appeared on the oscilloscope trace, alongside the MP. We tuned the ratio PP/MP from 0.1:1 to 4:1 (Fig. 1b, panels 2–6). At these conditions, the dynamics of laser–matter interaction became drastically different compared with above-described case of single-pulse interaction. First pulse (pre-pulse; Fig. 1b, panel 2), with the intensity ten times smaller compared with the MP, created the plasma plume during ablation of the edges of drilled hole by the wings of the spatial distribution of this pulse (see inset in Fig. 1a). The ablating species moved toward the optical axis of the hole; 8 ns later, the MP propagated through the area where some fastest particles of plasma had arrived, which led to harmonic generation. The harmonic emission was analyzed using the EUV spectrometer containing a cylindrical mirror and a 1200 grooves/mm flat field grating with variable line spacing. The spectrum was recorded by a micro-channel plate detector with the phosphor screen, which was imaged onto a charge-coupled device camera.

Note that the plasma cloud was very thin and approximately corresponded to the thickness of the targets (~ 0.1 mm). It means that the harmonic generation was carried out during interaction of the laser pulse with small amount of the potential emitters of coherent radiation. Previous studies of plasma harmonics were performed using significantly longer plasma plumes (0.5–5 mm)

Fig. 1 a Experimental arrangements for harmonic generation during ablation of thin films using the double-pulse scheme. *DDPB* driving double-pulse beam; *FL* focusing lens, *MP* main pulse, *PP* pre-pulse, *TT* thin target, *HB* harmonic beam, *S* slit, *EUVS* extreme ultraviolet spectrometer, *MB* main beam, *PB* pre-pulse beam. **b** Oscilloscope traces of double pulses at different ratios of pre-pulse and main pulse



[13–20]. Further, the short delay between pulses (8 ns) did not allow the whole cloud of ablated particles to propagate the distance equal to the radius of drilled hole ($\sim 40 \mu\text{m}$). These two obstacles considerably diminished the nonlinear optical response of the plasma medium. Nevertheless, we were able to observe the HHG even at these extremely unfavorable conditions.

Particularly, we obtained the harmonic generation in the case of indium and molybdenum drilled films. A specific pattern was observed in the case of 0.1-mm-thick In film, when the resonantly enhanced 13th harmonic dominated over the plasma emission spectrum. The generated spectrum also contained weak 11th and 15th harmonics

(Fig. 2a, second panel from the top). The harmonics were generated at a small ratio PP/MP (0.2:1) and were recognized by their small divergence compared with the plasma emission observed in the raw spectra. The growth of this ratio (0.7:1) led to strong plasma emission and disappearance of harmonics (Fig. 2a, upper panel). One can see in this spectrum the strong emission line ($4d^95s^2\ ^1S_0 \rightarrow 4d^95s^25p\ (^2D)\ ^1P_1$, $\lambda = 62.2 \text{ nm}$) in the vicinity of 13th harmonic ($\lambda = 61.7 \text{ nm}$). This ionic transition possessing high oscillator strength is assumed to be responsible for the enhancement of the 13th harmonic compared with the neighboring ones [21]. This emission line remained unchanged once we introduced the quarter-wave

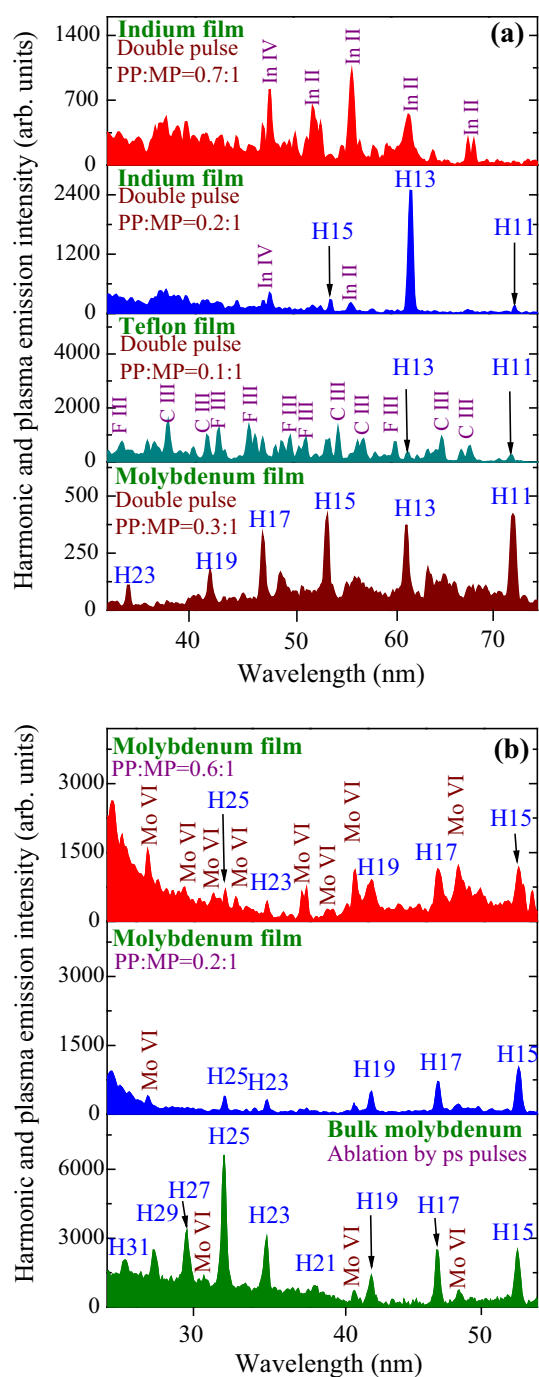


Fig. 2 **a** Harmonic and plasma spectra obtained during ablation (from top to bottom) of the indium film (PP/MP = 0.7:1 and 0.2:1), Teflon film (PP/MP = 0.1:1), and molybdenum film (PP/MP = 0.3:1). **b** Harmonic and plasma spectra obtained during ablation of the molybdenum film at different ratios of pre-pulse and main pulse (upper panel PP/MP = 0.6:1; middle panel PP/MP = 0.2:1). Bottom panel shows the harmonic spectrum obtained during ablation of 5-mm-long bulk Mo target by the 370-ps pulses (see text)

plate in the path of femtosecond pulse and changed the polarization from linear to circular, thus showing the incoherent properties of the 62.2 nm radiation. Contrary to

that, in the case of 0.2:1 ratio of two pulses, the harmonics disappeared from the spectra in the case of circular polarization of the driving pulses.

The strong plasma emission with the weak lower-order (H11–H15) harmonics in the case of double-pulse scheme was observed using some other metal films. Some non-metal films also showed similar behavior. Particularly, thin (0.2 mm) Teflon did not allow strong harmonic generation in a broad range of PP/MP ratios. Even at a small value PP/MP (0.1:1, Fig. 2a third panel from the top), the double-pulse beam produced a large amount of plasma emission. This emission was mostly assigned to the fluorine and carbon doubly charged ions, while weak lowest-order harmonics (H11 and H13) were appeared among the plasma lines. These harmonics were distinguished from the plasma emission by considerably smaller divergence.

Molybdenum film with 0.04 mm thickness showed the strongest harmonic spectrum among the metal film targets (Fig. 2a, bottom panel). The harmonics up to the 25th order were observed at the PP/MP ratios varying between 0.2:1 and 0.6:1 (Fig. 2b, two upper panels). Though the optimal ratio was close to 0.2:1, the growth of pre-pulse did not significantly suppress the harmonics but rather increase the plasma emission from highly charged molybdenum ions (Fig. 2b, upper panel).

The interesting peculiarity of harmonic spectrum from this film was a notable absence of the 21st harmonic (see Fig. 2a, bottom panel, b, two upper panels). Probably, some ionic transitions in the vicinity of this harmonic significantly changed the phase-matching conditions, which led to the suppression of the constructive accumulation of the H21 photons during propagation of the MP through the thin plasma.

To prove this assumption, we compared the harmonics generated in the drilled molybdenum film with the commonly used method of plasma formation by the picosecond pulse followed with propagation of the single femtosecond driving pulse, after the optimal delay, through the pre-formed extended plasma plume. We used the 370 ps uncompressed radiation from the same laser for the plasma formation. These 370-ps heating pulses were focused using a 200-mm-focal-length spherical lens inside the vacuum chamber contained a 5-mm-long Mo target to create the extended plasma plume. The intensity of heating picosecond pulses on the target surface was $4 \times 10^9 \text{ W cm}^{-2}$. The 70-fs driving pulses were used, after 43-ns delay from the beginning of ablation, for harmonic generation in the Mo extended plasma. The single driving pulses were focused onto the plasma from the orthogonal direction, at a distance of $\sim 100 \mu\text{m}$ above the target surface. The harmonic cutoff (H35) and conversion efficiency in that cases were reasonably larger compared with the case of the double-pulse beam propagated through the drilled Mo film. Note that in

the case of ablated bulk target, the H21 was also significantly suppressed (Fig. 2b, bottom panel), similar to the experiments with the thin film.

The strongest harmonics using double-pulse scheme were achieved in the case of 0.08-mm-thick polyethylene film (Fig. 3a, thick curve). The single-pulse scheme caused the appearance of strong emission assigned to the C II–C IV transitions (Fig. 3a, thin curve). Once we switched to the double-pulse scheme, the “clean” harmonic spectra were observed in a broad range of PP/MP ratios (Fig. 3b, four upper panels). The maximum harmonic yield was

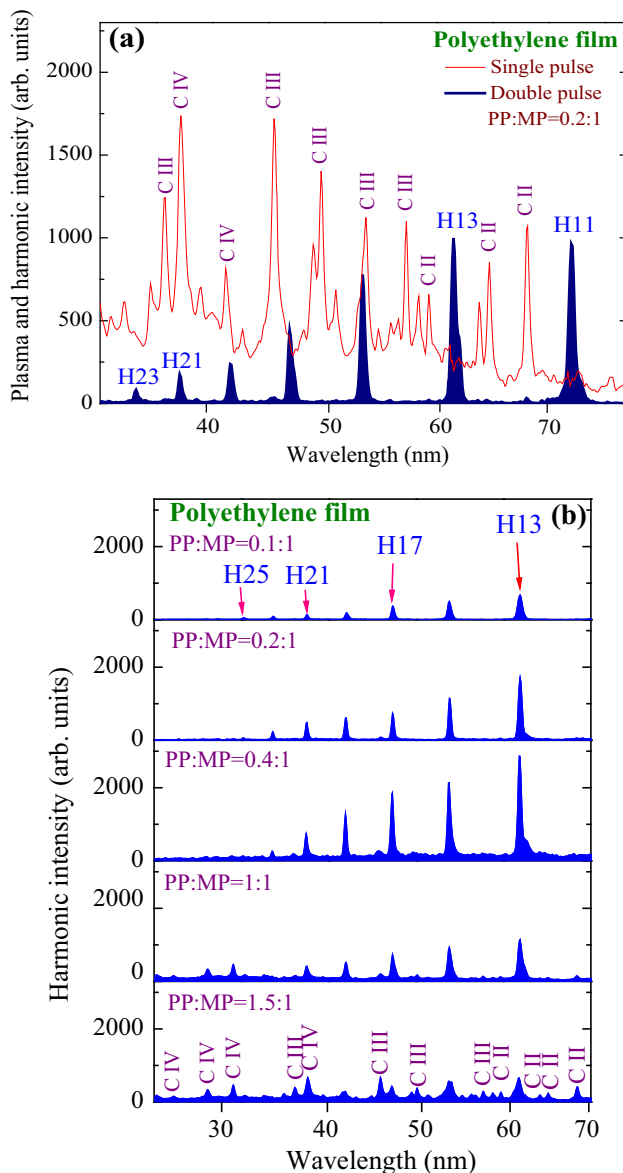


Fig. 3 **a** Plasma and harmonic spectra obtained during propagation of the laser radiation through the ablated polyethylene film in the case of single-pulse (*thin curve*) and double-pulse (*filled curve*) driving beam. **b** Harmonic spectra obtained from the drilled polyethylene film at different ratios of the pre-pulse and main pulse

obtained in the case of PP/MP = 0.4:1. The harmonics became significantly suppressed only at the 1.5:1 ratio between the pre-pulse and MP (Fig. 3b, bottom panel).

Similar features were observed in the case of another carbon-contained material, 0.1-mm-thick paper sheet. Strong plasma emission appeared from the C III and C IV ionic transitions alongside the harmonics at the PP/MP = 0.6:1 (Fig. 4a). The plasma emission was suppressed at the lower ratio of pulses (0.3:1, Fig. 4b), while keeping the same harmonic spectrum. The application of two-color scheme (802 nm + 401 nm), when the BBO crystal was inserted in the path of the focused 800-nm beam, showed the generation of even harmonics (H10–H16), alongside the odd ones. One can assume that the advanced properties of these two thin targets (polyethylene and paper) were related to the excellent features of carbon-

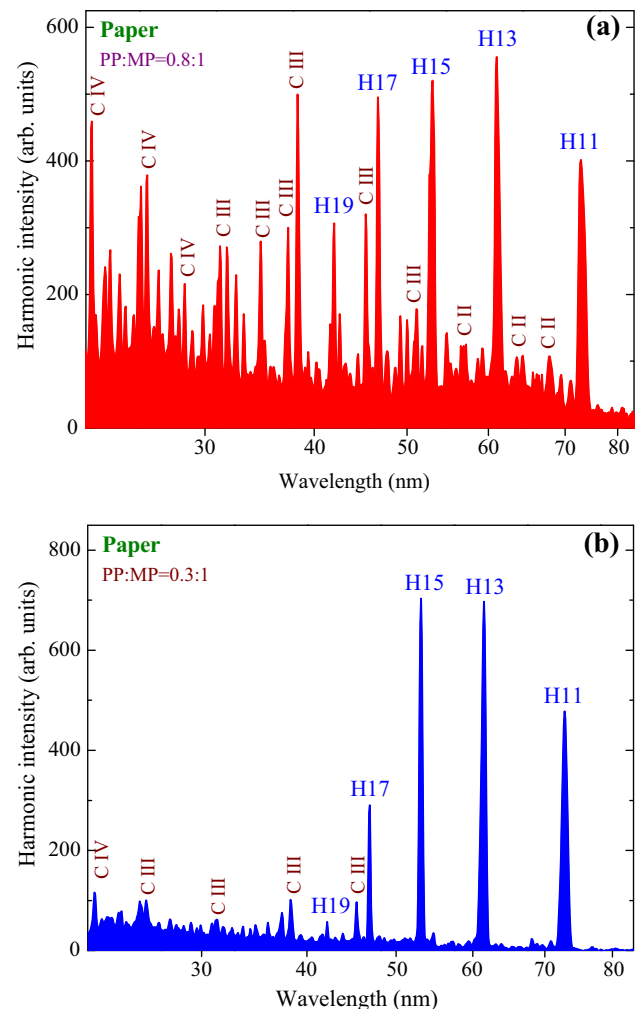


Fig. 4 Plasma and harmonic spectra obtained from the drilled paper sheet at different ratios of the pre-pulse and main pulse. **a** 0.8:1, **b** 0.3:1

contained plasma, which were proven during previous studies of plasma harmonics [15].

The proposed method allows a simplified method of HHG using thin samples, without the ablation using the additional picosecond pulses. At the same time, this technique could be applied for the direct observation of the HHG from the solids. Particularly, the ultrathin species, such as graphene sheets, could be directly probed by the femtosecond pulses taking the advantage of small absorption in this medium.

4 Conclusions

In conclusion, we have demonstrated the harmonic generation using the two femtosecond pulses propagated through the drilled thin films. The high-order harmonics of ultrashort pulses were observed in the case of double-pulse scheme while using various films (Mo, In, polyethylene, paper). The attractive properties of this method (simplicity, absence of additional source of heating radiation, and artificial optimization of plasma formation using the adjustment of the intensities of two pulses) show the possibility in application of this technique for the HHG in thin ablated films.

References

1. A. McPherson, G. Ginson, H. Jara, N. Johann, I.A. McIntyre, K. Boyer, C.K. Rhodes, *J. Opt. Soc. Am. B* **4**, 595 (1987)
2. M. Ferray, A. L'Huillier, X.F. Li, L.A. Lompré, G. Mainfray, G. Manus, *J. Phys. B At. Mol. Opt. Phys.* **21**, L31 (1988)
3. Y. Akiyama, K. Midorikawa, Y. Matsunawa, Y. Nagata, M. Obara, H. Tashiro, K. Toyoda, *Phys. Rev. Lett.* **69**, 2176 (1992)
4. C.-G. Wahlström, S. Borgström, J. Larsson, S.-G. Pettersson, *Phys. Rev. A* **51**, 585 (1995)
5. R.A. Ganeev, V.I. Redkorechev, T. Usmanov, *Opt. Commun.* **135**, 251 (1997)
6. G.I. Petrov, V. Shcheslavskiy, V.V. Yakovlev, I. Ozerov, E. Chelnokov, W. Marine, *Appl. Phys. Lett.* **83**, 3993 (2003)
7. V. Narayanan, R.K. Thareja, *Opt. Commun.* **260**, 170 (2006)
8. G. Khanarian, M.A. Mortazavi, A.J. East, *Appl. Phys. Lett.* **63**, 1462 (1993)
9. S.O. Konorov, D.A. Akimov, A.A. Ivanov, M.V. Alfimov, S. Botti, R. Ciardi, L. De Dominicis, L.S. Asilyan, A.A. Podshiv- alov, D.A. Sidorov-Biryukov, R. Fantoni, A.M. Zheltikov, *J. Raman Spectrosc.* **34**, 1018 (2003)
10. S. Konorov, A. Ivanov, M. Alfimov, A. Zheltikov, *J. Opt. A* **5**, 362 (2003)
11. Y. Nosaka, K. Tanaka, N. Fujii, *J. Appl. Polym. Sci.* **47**, 1773 (1993)
12. P.B. Corkum, *Phys. Rev. Lett.* **71**, 1994 (1993)
13. L.B. Elouga Bom, F. Bouzid, F. Vidal, J.-C. Kieffer, T. Ozaki, *J. Phys. B At. Mol. Opt. Phys.* **41**, 215401 (2008)
14. H. Singhal, V. Arora, B.S. Rao, P.A. Naik, U. Chakravarty, R.A. Khan, P.D. Gupta, *Phys. Rev. A* **79**, 023807 (2009)
15. Y. Pertot, L.B. Elouga Bom, V.R. Bhardwaj, T. Ozaki, *Appl. Phys. Lett.* **98**, 101104 (2011)
16. L.B. Elouga Bom, Y. Pertot, V.R. Bhardwaj, T. Ozaki, *Opt. Express* **19**, 3077 (2011)
17. S. Haessler, L.B. Elouga Bom, O. Gobert, J.-F. Hergott, F. Lepetit, M. Perdrix, B. Carré, T. Ozaki, P. Salières, *J. Phys. B At. Mol. Opt. Phys.* **45**, 074012 (2012)
18. M. Kumar, H. Singhal, J.A. Chakera, P.A. Naik, R.A. Khan, P.D. Gupta, *J. Appl. Phys.* **114**, 033112 (2013)
19. S. Haessler, V. Strelkov, L.B. Elouga Bom, M. Khokhlova, O. Gobert, J.-F. Hergott, F. Lepetit, M. Perdrix, T. Ozaki, P. Salières, *New J. Phys.* **15**, 013051 (2013)
20. R.A. Ganeev, M. Suzuki, H. Kuroda, *Phys. Plasmas* **21**, 053503 (2014)
21. R.A. Ganeev, M. Suzuki, T. Ozaki, M. Baba, H. Kuroda, *Opt. Lett.* **31**, 1699 (2006)